RESEARCH ARTICLE

Figures and figure supplements

Expression of modified FcγRI enables myeloid cells to elicit robust tumor-specific cytotoxicity

Leen Farhat-Younis *et al*.

Figure 1. IgM-induced signaling elicits cytotoxic response in macrophages and can be integrated to a CAR design. (**A**) Illustration of experimental setting. (**B**) B16F10 tumor size (mm^2) in mice following prophylactic immunization with MoDC pulsed with tumor cells coated with allogeneic IgG or IgM (n=4). (**C**) Mean percentages of B16F10 melanoma cells stained for Annexin V/PI incubated with allogenic IgG and IgM following incubation with MoDC (n=5). (**D–E**) Mean levels of Granzyme B and NO (**D**) and proinflammatory cytokines (**E**) in the supernatants of MoDC following overnight activation with

Figure 1 continued on next page

Figure 1 continued

IgG and IgM immune complexes (n=5). (**F**) Mean fluorescent intensity (MFI) of MAPK enzymes in MoDC following activation for 20 min with IgG and IgM tumor immune complexes (n=5). (**G**) Illustration representing CAR-macrophage design. (**H**) Confocal microscopy images of HEK293FT cells 24 hr post-transfection with CAR plasmids and membranous wasabi. (**I**) Representative FACS analysis of HEK239FT cells 24 hr post-transfection with CAR plasmids. Results are from one representative experiment out of at least three performed. Statistical significance was calculated using non-parametric t-test (* denote $p<0.05$, *** denote $p<0.001$, **** denote $p<0.0001$).

© 2024, BioRender Inc. Figure 1A, G was created using BioRender, and is published under a CC BY-NC-ND license. Further reproductions must adhere to the terms of this license.

Figure 2. scFv is not expressed by myeloid cells. (**A**) Confocal microscopy images of DC 2.4 cells 24 hr post-transfection with CAR plasmids and membranous wasabi. (**B**) Representative FACS analysis of DC 2.4 cells 24 hr post-transfection with CAR plasmids. (**C**) Percentages of transfected cells 24 hr post-transfection (n=4). (**D**) Confocal microscopy images of THP-1 cells 72 hr post lentiviral infection with CAR-C5aR-mCherry and tdTomato plasmids. (**E**) Percentages of transfected human cell lines 72 hr following transduction (n=4). (**F–G**) Representative confocal microscopy (**F**) and mean

Figure 2 continued on next page

Figure 2 continued

percentages (**G**) of cells expressing chimeric molecules 24 hr after transfection. (**H–I**) Representative confocal microscopy (**H**) and mean percentages of cells (**I**) expressing chimeric molecules 24 hr following transfection (n=4). Results are from one representative experiment out of at least three performed. Statistical significance was calculated using non-parametric t-test (** denote p<0.01, **** denote p<0.0001).

© 2024, BioRender Inc. Figure 2F, H was created using BioRender, and is published under a CC BY-NC-ND license. Further reproductions must adhere to the terms of this license.

Figure 2—figure supplement 1. scFv is not expressed by myeloid cells. (**A**) Confocal microscopy images of RAW264.7 cells transfected with scFv-based chimeric receptors. (**B–C**) Confocal microscopy images (**B**) and mean expression percentages (**C**) of HEK293FT and DC2.4 cells 24 hr post-transfection with TA99 scFv (n=4). (**D–E**) Confocal microscopy images of HEK293FT and DC 2.4 cells 24 hr post-transfection with αCD19 scFv (**D**) and with CD8-

Figure 2—figure supplement 1 continued on next page

Figure 2—figure supplement 1 continued

transmembrane portion only (**E**). Results are from one representative experiment out of at least three performed. Statistical significance was calculated using non-parametric t test.

© 2024, BioRender Inc. Figure 2—figure supplement 1B, D and E was created using BioRender, and is published under a CC BY-NC-ND license. Further reproductions must adhere to the terms of this license.

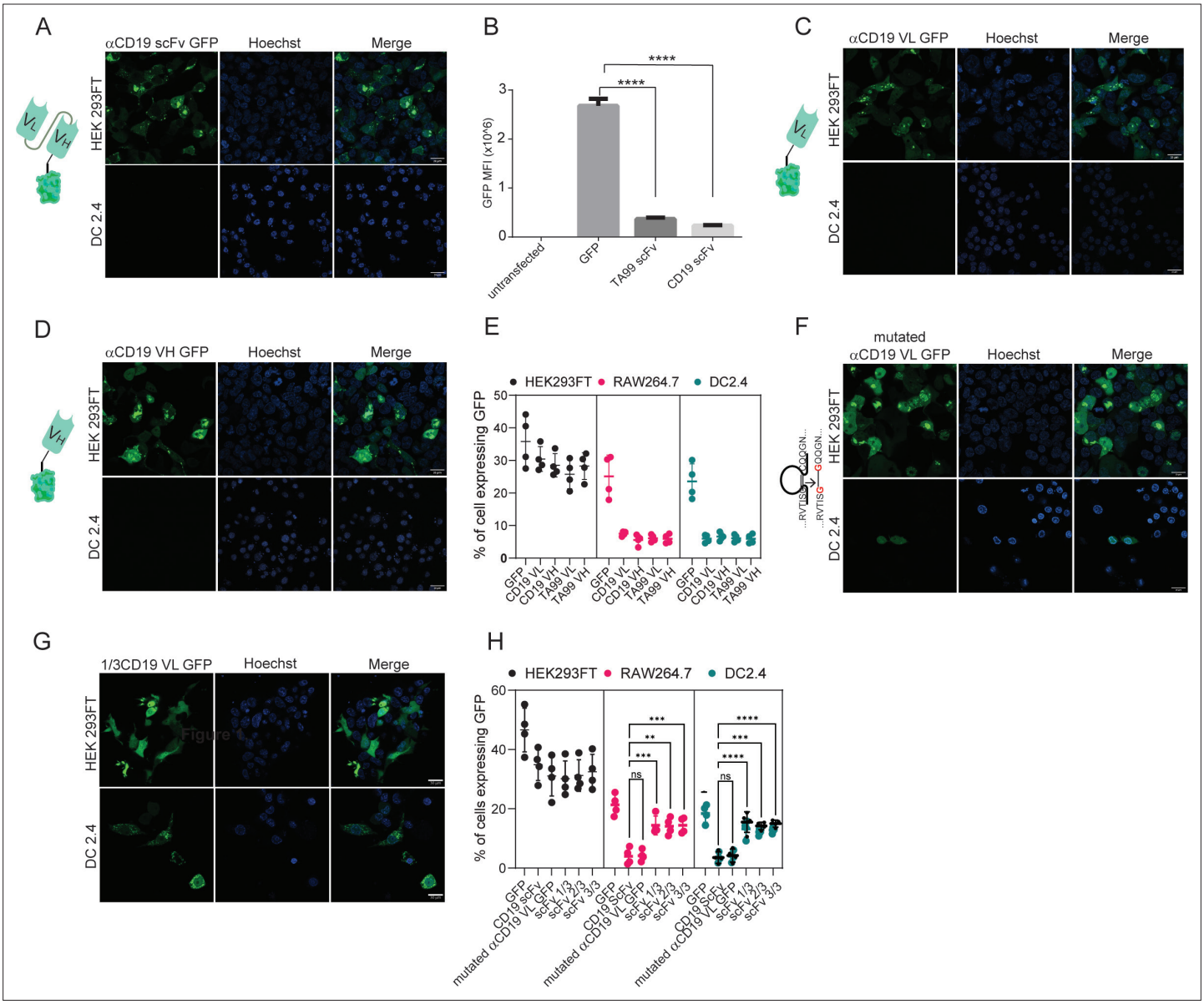

Figure 3. Both VH and VL domains prevent expression of ScFv in myeloid cells. (**A**) Confocal microscopy images of DC 2.4 cells 24 hr post-transfection with αCD19-scFv GFP plasmid. (**B**) Geometric mean of GFP-positive cells 24 hr post-transfection with different αCD19- and TA99- ScFv GFP constructs in DC2.4 (n=3). (**C**) Confocal microscopy images of HEK 293 FT and DC 2.4 cells 24 hr post-transfection with αCD19-variable light chain GFP plasmid. (**D**) Confocal microscopy images of HEK 293 FT and DC 2.4 cells 24 hr post-transfection with αCD19-variable heavy chain GFP plasmid. (**E**) Mean percentages of cells expressing scFv fragments 24 hr post-transfection (n=4). (**F**) Left: Illustration of mutated variable light chain. Right: Confocal microscopy images of HEK 293 FT and DC 2.4 cells 24 hr post-transfection with αCD19- mutated (linear) variable light chain. (**G**) Confocal microscopy images of HEK293FT and DC2.4 cells 24 hr post-transfection with 1/3 fragments of αCD19-variable light chain GFP plasmid. (**H**) Mean percentages of GFP-positive cells 24 hr post-transfection with different fragments of scFv-GFP in DC2.4 and RAW264.7 (n=4). Results are from one representative experiment out of at least three performed. Statistical significance was calculated using non-parametric t test (** denote p<0.01, *** denote p<0.001, **** denote p<0.0001).

© 2024, BioRender Inc. Figure 3A, C and D was created using BioRender, and is published under a CC BY-NC-ND license. Further reproductions must adhere to the terms of this license.

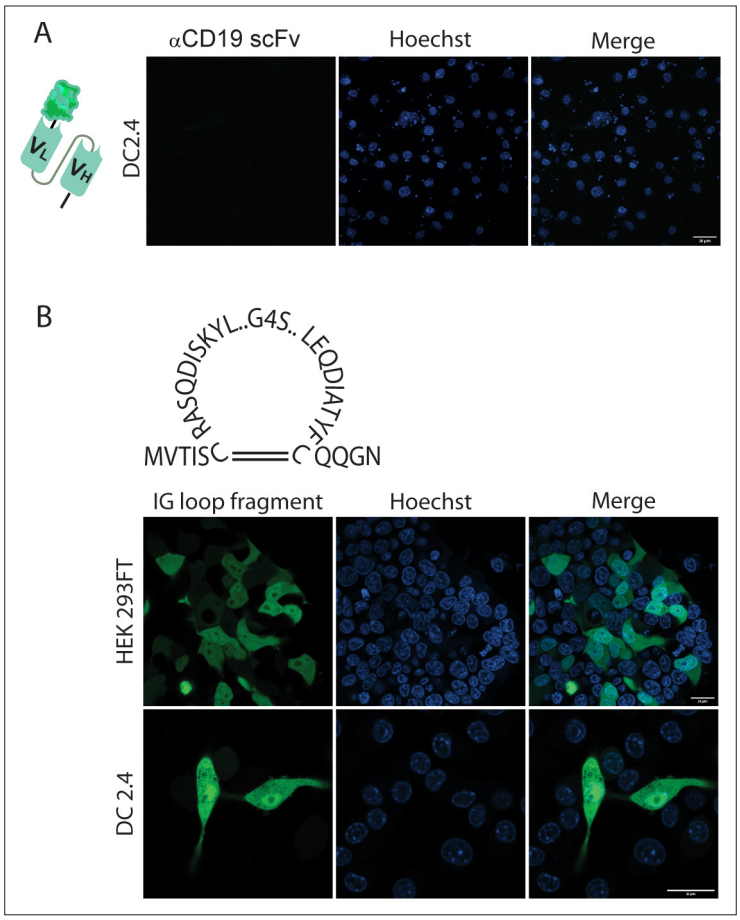

Figure 3—figure supplement 1. Immunoglobulin structure of scFv does not prevent degradation by myeloid cells. (**A**) Representative confocal images of DC 2.4 transfected with αCD19 scFv fused to GFP at the carboxyl end. (**B**) Upper: Illustration of immunoglobulin loop fragment GFP. Lower: Confocal microscopy images of HEK293FT and DC2.4 24 hr post-transfection with immunoglobulin loop fragment. Results are from one representative experiment out of at least three performed.

© 2024, BioRender Inc. Figure 3—figure supplement 1A was created using BioRender, and is published under a CC BY-NC-ND license. Further reproductions must adhere to the terms of this license.

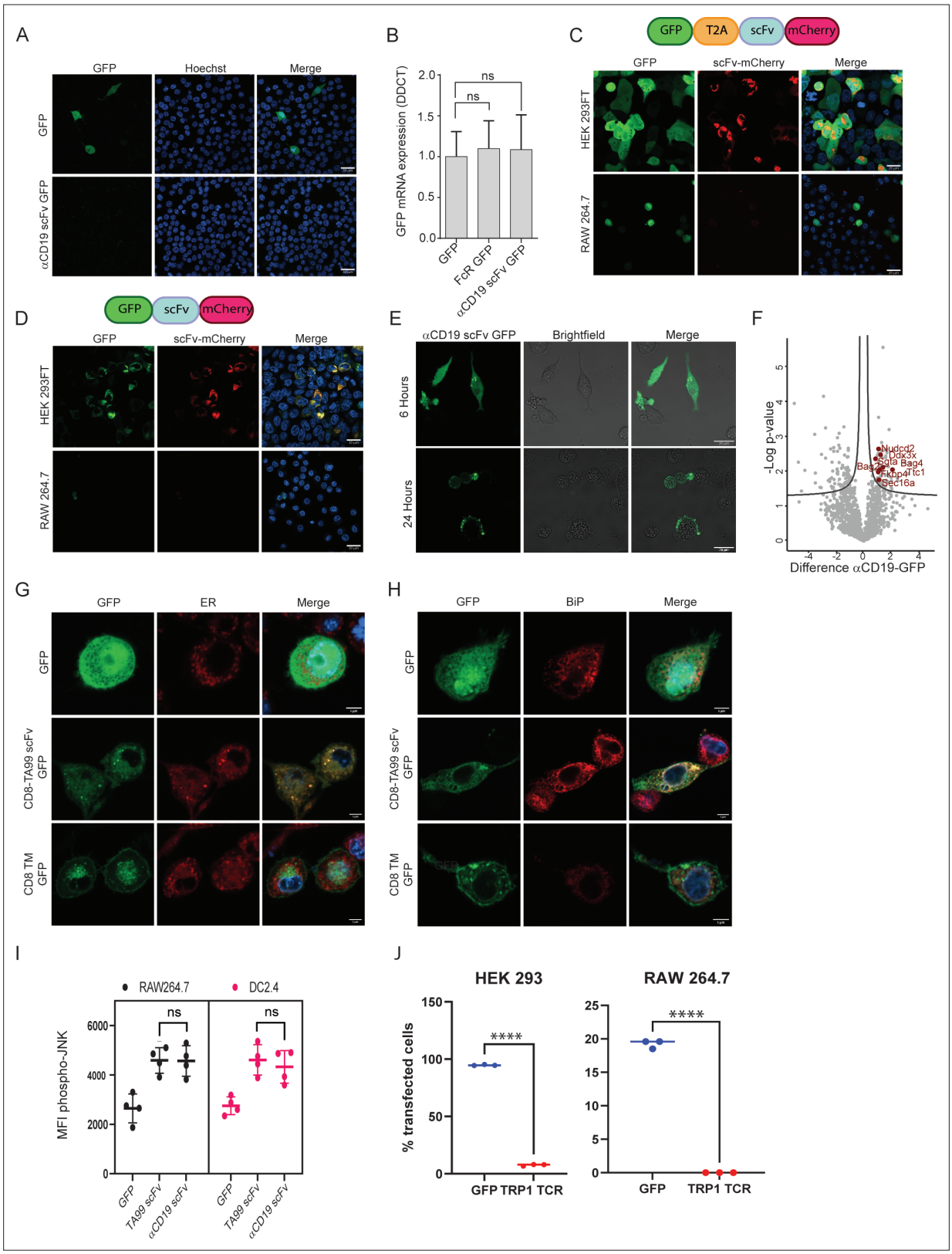

Figure 4. scFv fragments induce ER stress in myeloid cells. (**A**) Confocal microscopy imaging of RAW 264.7 24 hr post-transfection with linear mRNA vectors translating to GFP and αCD19-scFv GFP. (**B**) qPCR data showing relative mRNA levels in RAW 264.7 transfected with GFP, Fc receptor-GFP, and αCD19-scFv GFP (n=4). (**C**) Upper: Illustration of plasmid subunits. Lower: Confocal microscopy imaging of HEK293FT and RAW 264.7 24 hr post-transfection with T2A ribosomal skipping plasmid including ScFv. (**D**) Upper: Illustration of plasmid subunits. Lower: Confocal microscopy imaging of

Figure 4 continued on next page

Figure 4 continued

HEK293FT and RAW 264.7 24 hr post-transfection with plasmid not containing T2A. (**E**) Confocal microscopy images of RAW264.7 cells at 6 hr and 24 hr post-transfection with αCD19-ScFv GFP plasmid. (**F**) Volcano plot showing differentially expressed proteins αCD19 ScFv GFP and GFP in DC 2.4 cells. (**G**) Confocal microscopy images of DC 2.4 stained with an ER stain, 24 hr post-transfection with GFP, membranous TA99-ScFv GFP. (**H**) Confocal microscopy images of DC 2.4 stained for BiP 24 hr post-transfection. (**I**) Mean levels of phospho-JNK 6 hours following transfection (n=4). (**J**) Percentage of cells expressing GFP or TRP-TCR1 24 hr following transfection (n=3). Results are from one representative experiment out of at least three performed. Statistical significance was calculated using non-parametric t-test (**** denote $p<0.0001$).

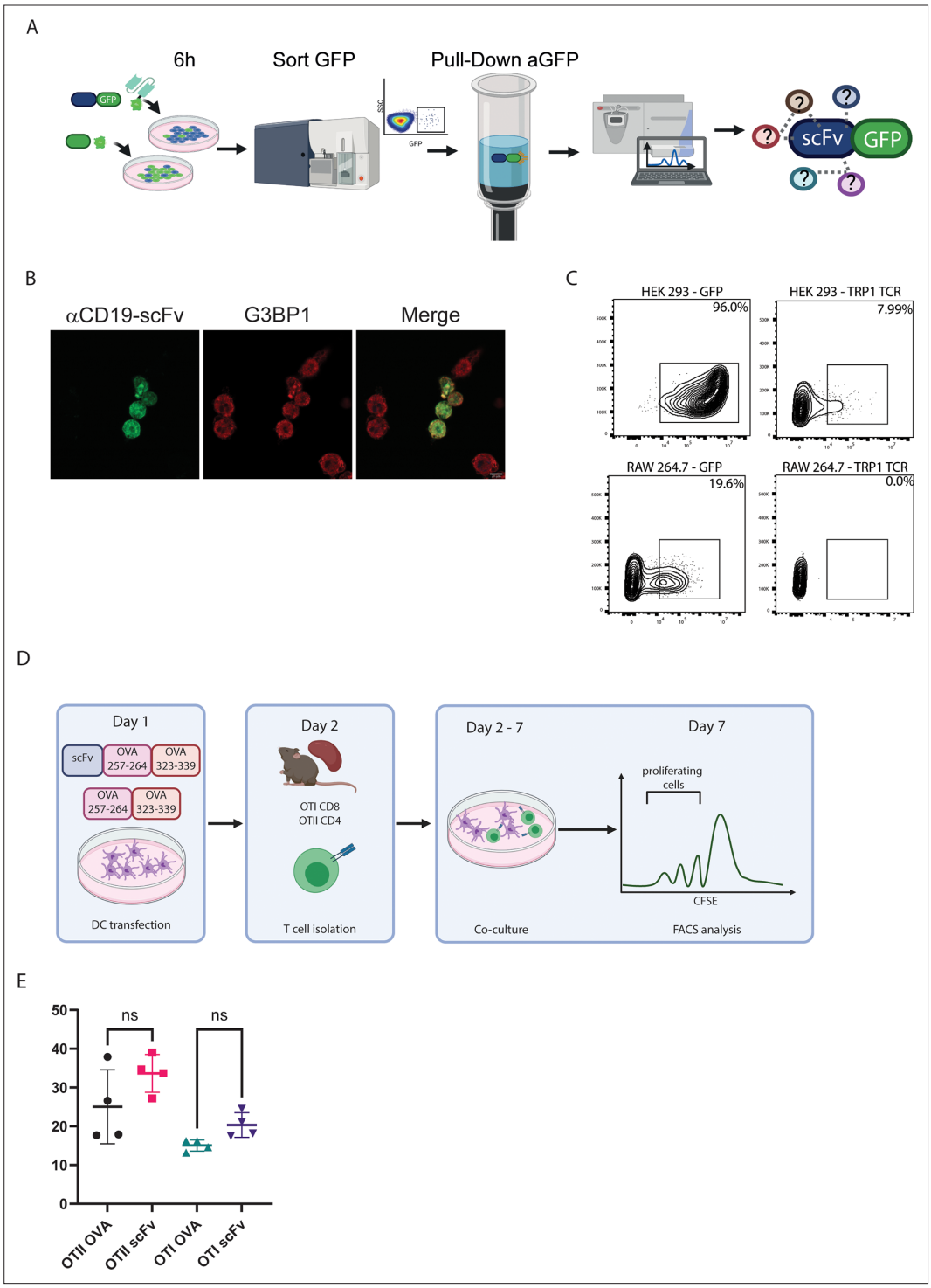

Figure 4—figure supplement 1. scFv induces ER stress response in myeloid cells. (**A**) Illustration of experimental design. (**B**) Confocal microscopy images with staining for G3BP1 in DC2.4 cells 6 hr post-transfection with αCD19 scFv. (**C**) Representative FACS analysis of HEK239FT and RAW 264.7 cells 24 hr post-transfection with TRP1-TCR. (**D**) Illustration of experimental design. (**E**) Representative analysis of CFSE dilution in $CD8^+$ and $CD4^+$ T cells following co-culture with ova conjugated scFv (n=4). Results are from one representative experiment out of at least three performed. Statistical significance was calculated using non-parametric t-test.

© 2024, BioRender Inc. Figure 4—figure supplement 1A, D was created using BioRender, and is published under a CC BY-NC-ND license. Further reproductions must adhere to the terms of this license.

Figure 5. FcγRI can provide a scaffold for incorporating IgM-induced signaling in myeloid cells and endows them with tumor cell-specific killing ability. (**A**) Illustration of chimeric Fcγreceptor design. (**B–C**) Representative FACS plots (**B**) and mean percentages (**C**) of RAW 264.7 cells expressing chimeric Fcγ receptors 24 hr after transfection (n=3). (**D**) Confocal microscopy images of RAW 264.7 cells 24 hr post-transfection with Fcγ receptors tagged with GFP and membrane-tagged tdTomato. (**E**) Mean percentages of BMDC 72 hr post lentivirus transduction with Fcγ receptors (n=4). (**F**) Confocal

Figure 5 continued on next page

Figure 5 continued

microscopy staining of GrB in RAW 264.7 cells co-cultured overnight with 4T1 cells expressing human HER2. (**G**) Mean counts of GrB in the synapse between transduced RAW 264.7 cells and the tumor cells (n=18). (**H**) IncuCyte analysis of human HER2$^+$ 4T1 cells growth following incubation with transduced RAW 264.7 cells (n=6). (**I**) Super-resolution microscopy of GFP-tagged chimeric FcγR and mCherry-tagged gamma chain. (**J**) IncuCyte analysis of human HER2$^+$ 4T1 cells growth following incubation with transduced RAW 264.7 cells (n=6). (**K**) Tumor size measurements (mm^2) in mice treated with mRNA transfected BMDC with and without antibody. Arrows point to subcutaneous injection of treated BMDC (n=5). (**L**) Mean percentages of CD3$^+$ out of CD45$^+$ cells in B16F10 tumors from day 26 (n=4). Results are from one representative experiment out of at least three performed. Statistical significance was calculated using non-parametric t test (** denote p<0.01, **** denote p<0.0001).

© 2024, BioRender Inc. Figure 5A was created using BioRender, and is published under a CC BY-NC-ND license. Further reproductions must adhere to the terms of this license.

Figure 5—figure supplement 1. FcγRI can be used as a scaffold to transmit IgM-induced signaling. (**A**) Representative confocal staining of Granzyme B in transduced RAW 264.7 cells incubated overnight with 4T1 cells expressing human HER2 antigen. (**B**) Super-resolution microscopy of RAW 264.7 cells transfected with chimeric FcγRI molecules as such, or one hour after addition of free antibody. (**C**) Illustration of receptor design. (**D**) Mean percentages of RAW 264.7 cells expressing chimeric receptor (n=4). (**E**) Representative microscopy of RAW 264.7 cells co-transfected with GFP-fused chimeric

Figure 5—figure supplement 1 continued on next page

Figure 5—figure supplement 1 continued

receptor and mCherry-membrane protein. (**F**) Super-resolution microscopy of RAW 264.7 cells transfected with chimeric FcγRI molecules as such, or one hour after addition of free antibodies. (**G**) Confocal microscopy staining of GrB in RAW 264.7 cells co-cultured overnight with 4T1 cells expressing human HER2. (**H**) Illustration of experimental setting. (**I**) Representative photomicrographs of tumor-bearing mice 26 days after tumor injection. Results are from one representative experiment out of at least three independent experiments performed.

© 2024, BioRender Inc. Figure 5—figure supplement 1C, H was created using BioRender, and is published under a CC BY-NC-ND license. Further reproductions must adhere to the terms of this license.